



A straightforward procedure to build a non-toxic relaxometry phantom with desired T1 and T2 times at 3T

Victor Fritz^{1,2,3} · Sabine Eisele¹ · Petros Martirosian¹ · Jürgen Machann^{1,2,3} · Fritz Schick¹

Received: 2 November 2023 / Revised: 1 May 2024 / Accepted: 3 May 2024
© The Author(s) 2024

Abstract

Objective To prepare and analyze soy-lecithin-agar gels for non-toxic relaxometry phantoms with tissue-like relaxation times at 3T.

Methods Phantoms mimicking the relaxation times of various tissues (gray and white matter, kidney cortex and medulla, spleen, muscle, liver) were built and tested with a clinical 3T whole-body MR scanner. Simple equations were derived to calculate the appropriate concentrations of soy lecithin and agar in aqueous solutions to achieve the desired relaxation times. Phantoms were tested for correspondence between measurements and calculated T1 and T2 values, reproducibility, spatial homogeneity, and temporal stability. T1 and T2 mapping techniques and a 3D T1-weighted sequence with high spatial resolution were applied.

Results Except for the liver relaxation phantom, all phantoms were successfully and reproducibly produced. Good agreement was found between the targeted and measured relaxation times. The percentage deviations from the targeted relaxation times were less than 3% for T1 and less than 6.5% for T2. In addition, the phantoms were homogeneous and had little to no air bubbles. However, the phantoms were unstable over time: after a storage period of 4 weeks, mold growth and also changes in relaxation times were detected in almost all phantoms.

Conclusion Soy-lecithin-agar gels are a non-toxic material for the construction of relaxometry phantoms with tissue-like relaxation times. They are easy to prepare, inexpensive and allow independent adjustment of T1 and T2. However, there is still work to be done to improve the long-term stability of the phantoms.

Keywords MRI Phantom · Relaxometry · T1 · T2 · 3T · Soy Lecithin

Introduction

Phantoms serve as substitutes for biological tissue and are indispensable tools in quantitative magnetic resonance imaging (qMRI) research. Gels with known (or even adjustable) tissue-like T1 and T2 relaxation properties are useful for

research, especially for developing and testing new pulse sequences and post-processing techniques [1, 2] as human volunteers are not always available for long test sessions. Since medical device-grade phantoms with desired relaxation properties are not present at all research sites, a protocol for flexible, homemade phantoms could be very useful. Ideally, the materials used to make the phantoms should be inexpensive, non-toxic, and easy to work with.

In particular, relaxometry phantoms that mimic tissue-like relaxation times attract the interest of researchers. Relaxation times T1 and T2 are intrinsic tissue properties that depend on tissue composition and microenvironment [3]. Changes in native T1 and T2 values are known as sensitive indicators of various pathologies, including cancer, cardiovascular abnormalities, and brain diseases [4]. To verify accurate and precise T1 and T2 measurements with MRI equipment, the availability of suitable test objects with predefined values is essential.

✉ Victor Fritz
victor.fritz@med.uni-tuebingen.de

¹ Section of Experimental Radiology, Department of Diagnostic and Interventional Radiology, University of Tübingen, Hoppe-Seyler-Str. 3, 72076 Tübingen, Germany

² Institute for Diabetes Research and Metabolic Diseases of the Helmholtz Centre Munich at the University of Tübingen, Tübingen, Germany

³ German Center for Diabetes Research (DZD), Neuherberg, Germany

Interestingly, there are only few approaches to the fabrication of phantoms with tissue-like relaxation times T1 and T2. Relaxometry phantoms proposed so far are typically two-component mixtures consisting of a gelling agent (e.g. agarose, agar) doped with paramagnetic salt (e.g. MnCl_2 , NiCl_2 , GdCl_3) [5–16]. Here, the paramagnetic salt generally serves as a T1-modifier and the gelling agent as a T2-modifier. Knowing the relaxivities (r_1, r_2) of each component, one can design a phantom material that has the desired relaxation times. The required concentrations of the respective substances can be calculated according to the following formulas described by Tofts et al. [8, 9]:

$$C_a = \frac{R2 - R2_w - (r_2^{(b)}/r_1^{(b)})(R1 - R1_w)}{r_2^{(a)} - (r_2^{(b)}/r_1^{(b)})r_1^{(a)}} \quad (1)$$

$$C_b = \frac{R1 - R1_w - (r_1^{(a)}/r_2^{(a)})(R2 - R2_w)}{r_1^{(b)} - (r_1^{(a)}/r_2^{(a)})r_2^{(b)}} \quad (2)$$

where C_a and C_b are the concentrations of component a and b, $r_1^{(a,b)}$ and $r_2^{(a,b)}$ are the relaxivities of component a and b, $R1_w$ and $R2_w$ are the relaxation rates of pure water, and $R1$ and $R2$ are the relaxation rates to be achieved.

It has been shown that those phantoms can be reproducibly produced and exhibit high temporal stability [7–9]. However, paramagnetic salts are toxic, which complicates the production, handling and disposal of these phantoms. Furthermore, the presence of paramagnetic salts can strongly affect the magnetic susceptibility of the phantom material [17]. This could lead to adverse effects, especially for gradient echo sequences, as undesirable magnetic field inhomogeneities occur depending on the geometry and composition of the phantom. Therefore, research is underway to find alternative, non-hazardous substances that can replace paramagnetic salt as a T1 modifier and allow phantoms to be produced without safety and toxicity issues [18].

In this context, Sękowska et al. [19] presented MRI phantoms based on non-toxic detonation diamond nanoparticles (DND). The phantoms composed of agar, carageen, and DND particles suspended in dimethyl sulfoxide have been shown to successfully mimic the relaxation times of liver tissue. However, the data from the study suggests that phantoms with T1 values above 950 ms cannot be fabricated, at least not with the fabrication method presented—which is a disadvantage, as many tissues (e.g. gray matter, kidney, spleen, etc.) have T1 values in the range of 1000–2000 ms and therefore cannot be covered.

Another relatively new and promising approach is the use of soy lecithin in MRI phantoms. Soy lecithin is a naturally occurring emulsifier that has recently been found

to alter the relaxation times and diffusion properties of water [20, 21]. In addition, soy lecithin is inexpensive, readily available and non-toxic, making it ideal for phantom manufacturing. Therefore, it is obvious to use and test soy lecithin for the preparation of relaxometry phantoms, which was also the motivation for this work.

In the present work, soy-lecithin-agar gels were prepared and evaluated as an alternative phantom material for the construction of relaxometry phantoms with tissue-like relaxation times. Special attention was paid to an understandable presentation of the phantoms' development and fabrication process. Test phantoms mimicking the relaxation times of different tissue types were evaluated for their correctness (agreement between measured and targeted values), reproducibility and temporal stability.

Methods

Study design

Before phantom fabrication can begin, relaxivities r_1 and r_2 of soy lecithin and agar have to be determined (see Eqs. 1 and 2). For this purpose, pure aqueous soy lecithin solutions and pure agar gels of different concentrations (0, 1, 2, 3, 4, 5%) were prepared and examined using T1- and T2 mapping techniques.

Furthermore, it has to be ensured that the two substances are compatible and retain their effect even when mixed. A change in relaxivity as a function of the concentration of the other substance would make it impossible to apply simple Eqs. (1, 2) for determination of concentrations and thus produce correct phantoms. At least, the T1 modifier should have stable longitudinal relaxivity r_1 and the T2 modifier should have stable transverse relaxivity r_2 . To verify this, relaxivities of soy-lecithin were measured in the presence of different concentrations of agar (1%, 2%, 3%, 4%), while agar-relaxivities were measured in the presence of different concentrations of soy lecithin (1%, 2%, 3%, 4%).

After the preliminary experiments, test phantoms were designed to match the relaxation times T1/T2 of different tissues: grey matter (1820 ms/99 ms [3]), white matter (1084 ms/69 ms [3]), kidney cortex (1142 ms/76 ms [22]), kidney medulla (1545 ms/81 ms [22]), spleen (1328 ms/61 ms [22]), liver (812 ms/42 ms [3]), and muscle (1295 ms/34 ms [22]). Using the previously determined relaxivities and Eqs. 1 and 2, the appropriate concentrations of soy-lecithin and agar were calculated to achieve the desired T1 and T2 values. For the relaxation rates of pure water, the values $R1_w = 2950$ ms and $R2_w = 2000$ ms were used (determined by several preliminary measurements).

The phantoms were tested for correctness (agreement between measured and target values), reproducibility and

temporal stability. For this, all phantoms were prepared three times, independently on different days and examined on the day of preparation and 4 weeks after preparation. Possible mold growth was monitored by visual inspection of the samples during the 4-week study period. In addition, the samples were checked for homogeneity and the absence of air bubbles. Air bubbles are problematic because they cause magnetic field distortions that lead to susceptibility artifacts [15].

Preparation of the phantoms

Phantoms were prepared as follows (Fig. 1): First, the appropriate amount of soy lecithin (Carl Roth, Karlsruhe, Germany) was dissolved in demineralized water (Carl Roth, Karlsruhe, Germany) under magnetic stirring at 650 rpm for 10 min. Agar (Agar powdered pure, food grade, Pan-Reac-AppliChem-ITW Reagents, Darmstadt, Germany) was then stirred into the soy lecithin solution and the mixture was boiled using a microwave heater until the solution was clear and homogeneous. The solutions were then filled into sterilized polypropylene tubes (50 ml, Greiner Bio-One, Frickenhausen, Germany) and cooled to room temperature for gelation. High viscosity solutions were sonicated with an ultrasonic homogenizer (Hielscher Ultrasonics, Teltow, Germany) to remove air bubbles prior to solid gel formation. Pure aqueous soy lecithin solutions and agar gels of different concentrations (0, 1, 2, 3, 4, 5%) were prepared by the same procedure without addition of the other substance.

For the measurements, the samples were fixed in water-filled MR-compatible housings (Fig. 2a–b): The measurements to determine the individual relaxivities of soy lecithin

and agar as well as for the final test phantoms were performed using a cylindrical housing that can hold up to 7 tubes. In contrast, due to the large number of samples, the compatibility measurements of soy lecithin and agar were carried out using a larger square housing that can hold up to 16 phantoms.

All phantoms were stored in the scanner room for at least 6 h before measurements to ensure that the temperature of the samples could stabilize and adapt to the ambient temperature. Between measurements, the samples were stored in the dark in a laboratory cabinet at a room temperature of approx. 21 °C.

Data acquisition and analysis

Measurements were performed on a clinical 3.0 Tesla whole-body MR scanner (MAGNETOM Prisma^{fit}, Siemens Healthcare, Erlangen, Germany) with a 20-channel head coil at 21 °C ± 0.5 °C.

Relaxivity measurements of soy lecithin and agar in the mixture (compatibility measurements) were performed using an 18-channel body array coil, as the square housing containing all samples did not fit into the head coil. The corresponding measurement setups are shown in Fig. 2c–d. All data were processed and analyzed offline using in-house developed software (MATLAB, MathWorks, Natick, MA).

T1 and T2 measurements were performed with the following parameters: matrix = 128 × 128, FOV = 200 × 200 mm, slice thickness = 5 mm, number of slices = 1, slice in coronal plane, positioned in the center of the samples.

T1 was measured using a single slice inversion recovery turbo spin echo pulse sequence (IR-TSE) with TR of

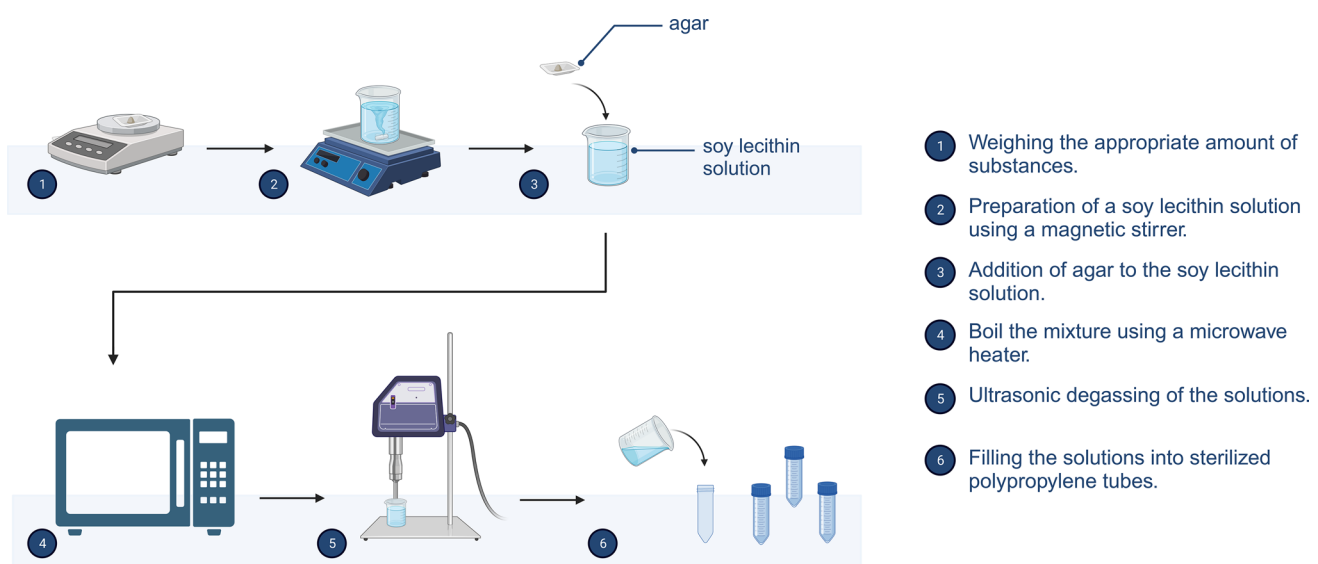


Fig. 1 Schematic representation of the manufacturing process of the soy-lecithin-agar phantoms. Created with [BioRender.com](https://www.biorender.com)

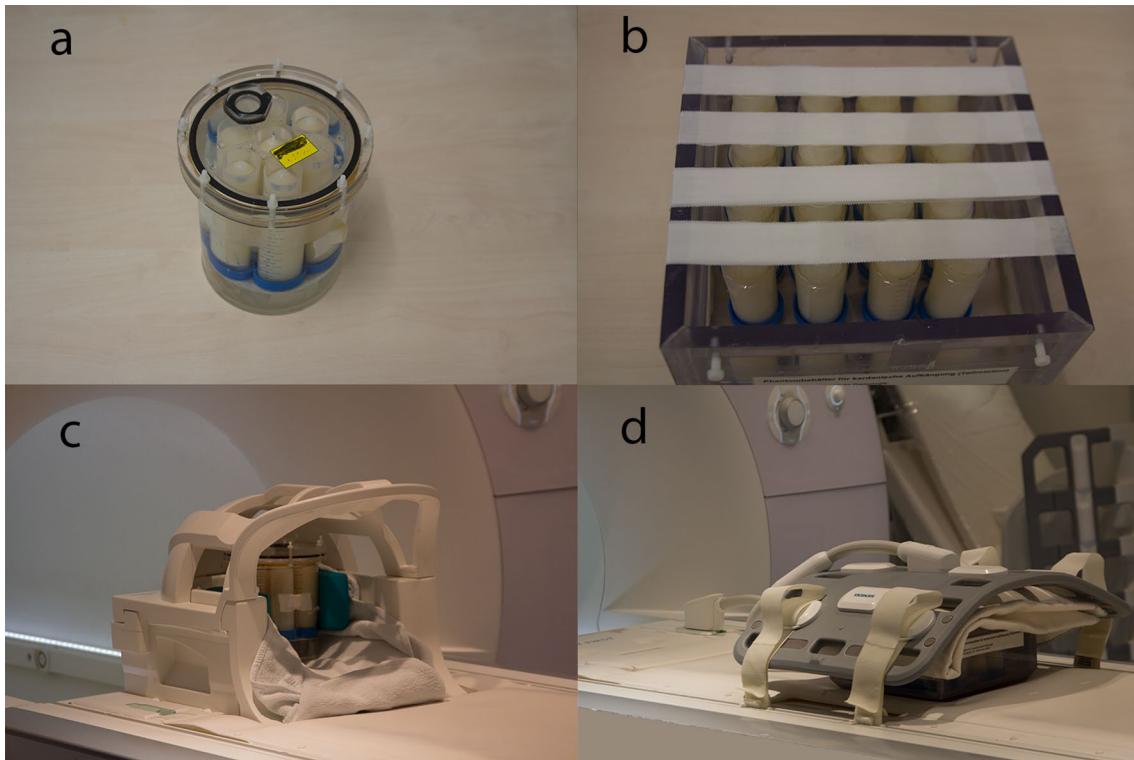


Fig. 2 Photographs of the water-filled sample tube housings: **a** cylindrical housing with 7 sample tubes **b** larger square housing with 16 sample tubes. Photographs of the measurement setup on a clinical 3T whole-body MR scanner: **c** the cylindrical housing with 7 sample

tubes was scanned using a 20-channel head coil **d** the square housing with 16 sample tubes was scanned using an 18-channel body array coil

10,000 ms and TE of 9.9 ms. Images were acquired for 9 different TIs in the range of 25–6400 ms (logarithmically equally spaced). T1 maps were calculated from the acquisitions with multiple TIs by pixel-wise monoexponential fitting of signal intensities (SI): $SI = SI_0 (1 - a \exp(-TI/T1) + \exp(-TR/T1))$ [23].

T2 was measured in the same slice using a multi-echo CPMG spin echo pulse sequence with a TR of 6000 ms and 32 TEs ranging from 10 to 320 ms (equally spaced). Since soy lecithin has a relatively small effect on T2, the T2 decay for the pure soy lecithin solutions (without agar) was sampled for longer TEs in the range of 50–1600 ms (equally spaced). T2 maps were calculated on a pixelwise basis by monoexponential fitting of the measured SI's: $SI = SI_0 \exp(-TE/T2) + c$ [22]. All signal values were noise corrected before fitting.

Relaxation times (T1, T2) and relaxation rates ($R1 = 1/T1$, $R2 = 1/T2$) of each sample were determined from circular regions of interest in the calculated parametric maps. Relaxivities were calculated from the linear regression of the relaxation rates on the concentration of the substance: $R_{1,2} = r_{1,2} \cdot [\text{concentration}] + c$. The slope of the line represents the relaxivity $r_{1,2}$.

A 3D T1-weighted gradient echo sequence (VIBE) with high spatial resolution was applied to examine the phantoms for homogeneity and the absence of air bubbles. Acquisition parameters include: TR = 6.3 ms, TE = 2.46 ms, FOV = 256 × 256, spatial resolution = 0.5 × 0.5 × 0.5 mm, number of slices = 10, coronal planes.

Results and discussion

First, the relaxation rates R1 and R2 of pure aqueous soy lecithin solutions and pure agar gels were measured at concentrations up to 5%. For both soy lecithin and agar, the relaxation rates showed a linear correlation with concentration (Fig. 3). Relaxivities r_1 and r_2 calculated using a linear fit gave $r_{1,\text{lecithin}} = 0.112 \text{ s}^{-1} \cdot \text{wt.}\%^{-1}$ ($R^2 = 0.99$), $r_{1,\text{agar}} = 0.039 \text{ s}^{-1} \cdot \text{wt.}\%^{-1}$ ($R^2 = 0.99$), $r_{2,\text{lecithin}} = 0.68 \text{ s}^{-1} \cdot \text{wt.}\%^{-1}$ ($R^2 = 0.99$), and $r_{2,\text{agar}} = 5.71 \text{ s}^{-1} \cdot \text{wt.}\%^{-1}$ ($R^2 = 0.99$), which is in good agreement to previous work [20].

Secondly, soy lecithin and agar were found to retain their effect even when mixed. Table 1 lists the relaxivities of soy lecithin as a function of agar concentration.

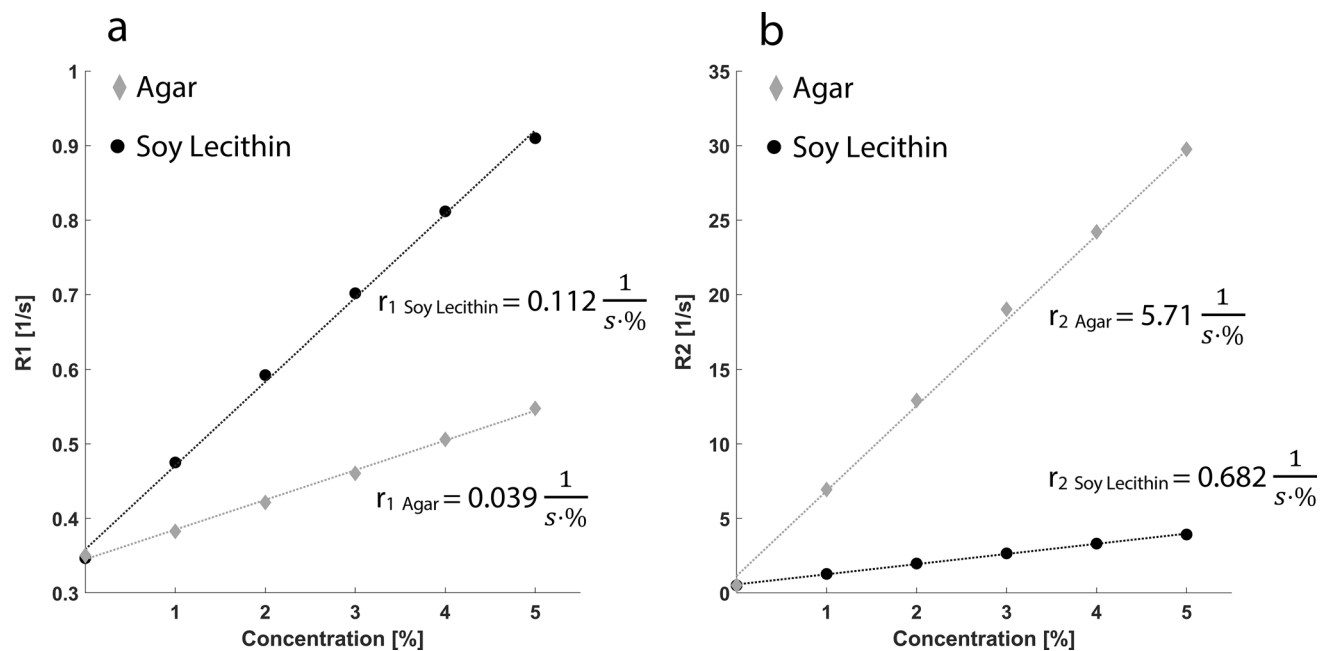


Fig. 3 Relaxation rates R1 (a) and R2 (b) of aqueous solutions as a function of soy lecithin and agar concentration, respectively

Table 1 Relaxivities r_1 and r_2 of soy lecithin in the presence of different agar concentrations. To measure the relaxivities of soy lecithin, the soy lecithin concentration was varied between 0%–4% (in steps of 1%) while the agar concentration was kept constant

Agar [%]	Soy lecithin			
	r_1 [$s^{-1}\cdot wt.\%^{-1}$]	R^2	r_2 [$s^{-1}\cdot wt.\%^{-1}$]	R^2
0	0.112	0.99	0.68	0.99
1	0.117	0.99	0.70	0.99
2	0.117	0.99	0.68	0.98
3	0.119	0.99	0.77	0.96
4	0.114	0.99	0.74	0.90
Mean	0.116	–	0.71	–

It becomes clear that both, r_1 and r_2 , hardly change in the presence of agar. Relaxivities showed little variation in the range of 0.112–0.119 $s^{-1}\cdot wt.\%^{-1}$ for r_1 and 0.68–0.77 $s^{-1}\cdot wt.\%^{-1}$ for r_2 , respectively. Similarly, agar relaxivities remained nearly constant in the presence of soy lecithin (Table 2). Relaxivities varied between 0.027–0.039 $s^{-1}\cdot wt.\%^{-1}$ for r_1 and 5.60–5.88 $s^{-1}\cdot wt.\%^{-1}$ for r_2 , respectively.

After determining the relaxivities and confirming the compatibility of soy lecithin and agar, the preparation of test phantoms mimicking organ related relaxation times was performed. For the relaxivities, the mean values $r_{1,lecithin} = 0.116 s^{-1}\cdot wt.\%^{-1}$, $r_{1,agar} = 0.033 s^{-1}\cdot wt.\%^{-1}$, $r_{2,lecithin} = 0.71 s^{-1}\cdot wt.\%^{-1}$, and $r_{2,agar} = 5.78 s^{-1}\cdot wt.\%^{-1}$ (see Table 1 and 2) were used in the following.

Table 2 Relaxivities r_1 and r_2 of agar in the presence of different soy lecithin concentrations. To measure the relaxivities of agar, the agar concentration was varied between 0%–4% (in steps of 1%), while the soy lecithin concentration was kept constant

Soy lecithin [%]	Agar			
	r_1 [$s^{-1}\cdot wt.\%^{-1}$]	R^2	r_2 [$s^{-1}\cdot wt.\%^{-1}$]	R^2
0	0.039	0.99	5.71	0.99
1	0.033	0.95	5.88	0.99
2	0.032	0.97	5.60	0.99
3	0.027	0.98	5.83	0.99
4	0.033	0.99	5.87	0.99
Mean	0.033	–	5.78	–

Substituting the calculated relaxivities into Eqs. 1 and 2 yields the following relationship between agar or soy lecithin concentration and desired relaxation times:

$$C_{Agar} = \frac{180}{T2[ms]} - \frac{1100}{T1[ms]} + 0.28 \quad (3)$$

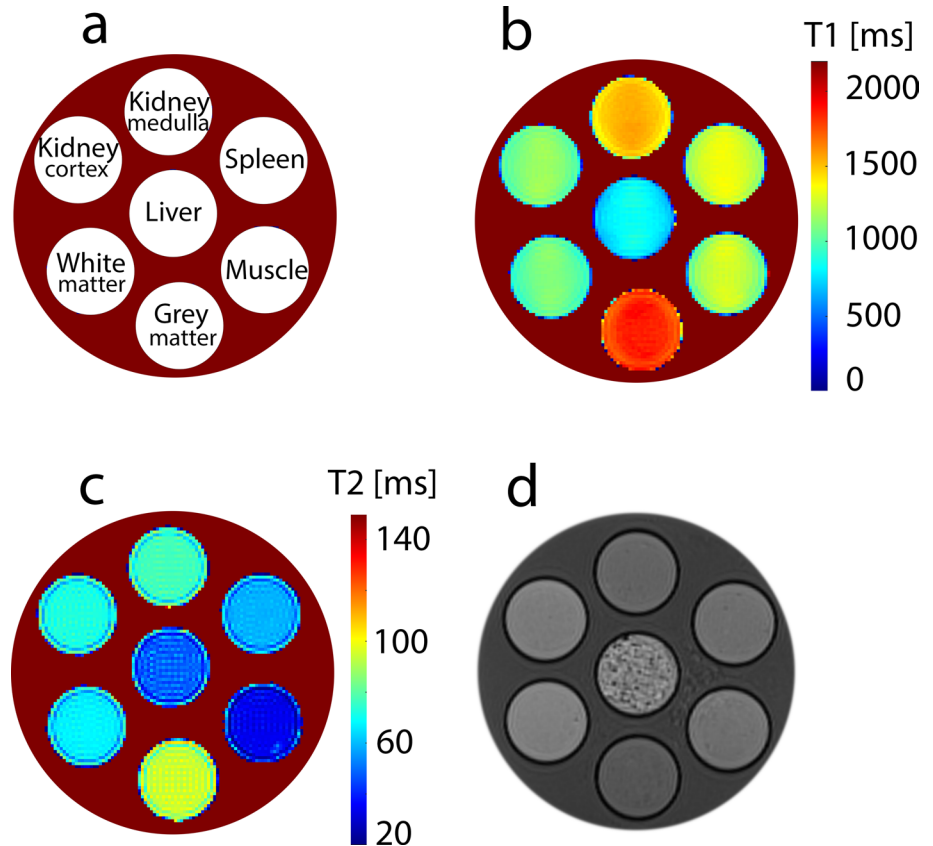
$$C_{Lecithin} = \frac{8930}{T1[ms]} - \frac{51}{T2[ms]} - 3 \quad (4)$$

Using these equations, samples were produced with relaxation times corresponding to the T1 and T2 times published in the literature for gray and white matter, kidney cortex and medulla, spleen, muscle, and liver. Table 3 provides an overview of the concentrations of soy lecithin

Table 3 Overview of the concentrations of soy lecithin and agar used and the targeted and measured T1 and T2 times of the test phantoms. The mean value and the standard deviation over the three measured phantom batches are shown

	T1 [ms]		T2 [ms]		Soy lecithin [%]	Agar [%]
	Target	Measured	Target	Measured		
Gray matter	1820	1850 ± 12	99	93 ± 3	1.39	1.49
White matter	1084	1093 ± 4	69	66 ± 2	4.50	1.87
Kidney cortex	1142	1159 ± 10	76	72 ± 2	4.15	1.69
Kidney medulla	1545	1539 ± 17	81	75 ± 3	2.15	1.79
Spleen	1328	1318 ± 23	61	58 ± 1	2.89	2.40
Muscle	1295	1262 ± 16	34	34 ± 1	2.40	4.72
Liver	812	834 ± 16	42	56 ± 6	6.78	3.21

Fig. 4 Parametric maps of test phantoms mimicking relaxation times of different tissues (grey matter, white matter, kidney cortex, kidney medulla, spleen, muscle, liver). **a** Representation of the positions of the test phantoms in the cylindrical measuring housing. **b** Parametric map of T1 times. **c** Parametric map of T2 times. **d** 3D T1-weighted image with high spatial resolution of test phantoms mimicking relaxation times of different tissues. With the exception of the liver phantom, all phantoms were homogeneous and showed little to no air bubbles. In contrast, the liver phantom had an inhomogeneous or brittle structure with many air bubbles



and agar used, as well as the targeted and measured T1- and T2 times. The corresponding T1- and T2 maps can be seen in Fig. 4a–c. Good agreement was found between the measured and targeted relaxation times. The largest deviations occurred for the liver phantom, where the percent deviation from the T1 set point was 2.7% and from the T2 set point was 32.5%. For all other phantoms, the percentage deviations from target relaxation times were less than 3% for T1 and less than 6.5% for T2, which is comparable to phantoms made with paramagnetic salts [15, 16]. In addition to the acceptable correspondence between calculated relaxation times and measured values, the reproducibility of the manufacturing process and resulting relaxation times T1 and T2 seems also sufficient for most

applications, as shown by the relatively small standard deviations across the three batches (Table 3).

3D T1-weighted images with high spatial resolution showed that the samples, with the exception of the liver phantom, were quite homogeneous and contained little to no air bubbles (Fig. 4d). Only the liver phantom had an inhomogeneous or brittle structure and showed significant air bubbles. Even degassing with ultrasound could not remove those air bubbles. This can be explained by the comparatively high concentrations of soy lecithin and agar required to prepare the liver phantom (see Table 3). The combination of high soy lecithin (> 6%) and high agar (> 3%) concentration results in a very viscous mixture, which in turn favors the entrapment of air bubbles

that form during the heating process. The resulting low homogeneity of the sample could also be the reason for the relatively high deviation between measured and target T2 time (32.5%) in the liver phantom. This indicates that gels mimicking tissues that have both short T1- and T2 times (eg. Liver, myocardial tissue) are problematic, as high concentrations of agar and soy lecithin are required. Evacuation of the surroundings of highly viscous gels could help to reduce or avoid air bubbles. However, this would require additional equipment and an additional preparation step.

The temporal stability of the phantoms was evaluated after a storage period of 4 weeks. Unfortunately, the phantoms were unstable over time, which was particularly reflected in the T1 times. Across all batches, the T1 times of all phantoms decreased significantly compared to the first measurement (Fig. 5a). The changes in T2 times were not quite as pronounced, but here too most phantoms showed a deviation from the initial measurement (Fig. 5b).

One possible reason for the altered relaxation behavior of the phantoms could be biodegradation by microorganisms. Without suitable additives, agar gels provide an ideal nutrient medium for fungi and bacteria [24], which biodegrade the phantom material over time and thus also alter MR properties. This could also be observed

macroscopically on some phantoms by means of mold growth (Fig. 5c).

The limited temporal stability of the soy-lecithin-agar phantoms is a major drawback compared to previously proposed phantoms using paramagnetic salts for T1 or T2 modification. Solutions with inorganic substances are stable for a long time without significant change in relaxation times [7]. This feature is very important when phantoms are employed for reproducibility measurements in multicenter studies where measurements are carried out over several weeks or even months.

To increase the biostability of soy-lecithin-agar phantoms and thus prevent microbial growth, preservatives such as fungicides and or bactericides can be used. It has been shown that the addition of these agents can maintain the stability of agar phantoms for up to 2 years [25]. However, most of the effective agents are quite toxic, which militates their use as it is contrary to the motivation of this study (production of relaxometry phantoms without toxic or questionable substances). Other preservatives such as citric acid or sodium sulfite, which are mainly used in the food industry [26], are harmless, but change the pH of the medium. Changing the pH would also be unfavorable since pH affects not only the properties of agar gels but also the micelle

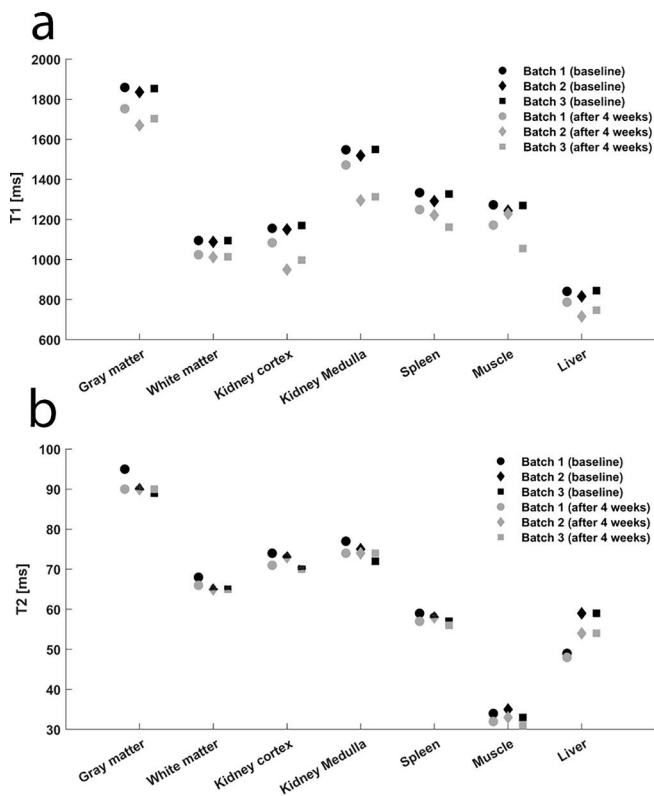


Fig. 5 To evaluate the temporal stability of the test phantoms, T1 and T2 measurements were repeated after 4 weeks under the same conditions. **a** Comparison of T1 times measured at baseline and after 4



weeks. **b** Comparison of T2 times measured at baseline and after 4 weeks. **c** Photograph of the test phantoms (batch 1) after a storage period of 4 weeks—mold growth is clearly visible on some phantoms

formation of soy lecithin molecules [27–29]. Soy lecithin is an amphiphilic molecule that forms micelles in aqueous solutions, the number, type and shape of which depend on various environmental parameters (pH, temperature, etc.) [27, 28]. This means that a preservative that affects the pH also changes the microstructure of the phantoms and thus their MR properties. It is still a challenge to find a suitable non-toxic preservative that will ensure the stability of the phantoms without compromising the effect of soy lecithin and agar. A number of systematic measurements are needed that are beyond the scope of this work but are planned for future studies. Another potential way to increase temporal stability is sterilization of the water or autoclaving the entire gels or UV irradiation of the phantoms. In this context, sensitivity of the organic substances to heat must be considered.

The temperature dependence of relaxation properties of the proposed gels has not been investigated so far. Knowledge of the temperature dependence can be important to account for temperature-related measurement deviations in practical usage of the phantoms. Furthermore, there is unpredictable dependence of relaxation on the magnetic field strength. In this study, the soy lecithin agar phantoms were examined at a field strength of 3T only. Further studies are needed to investigate their properties at higher and lower field strengths. Effects of different approaches for relaxometry (pulse sequences and data processing) is also an interesting area of research. It is a well-documented issue that relaxation times measured with different methods can vary considerably, even in the same subjects examined with the same MRI system [23, 30]. Further work will investigate whether similar variations in the relaxation times measured with different relaxometry approaches can also be observed in the soy-lecithin-agar phantoms.

While the soy-lecithin-agar phantoms effectively mimic desired relaxation times and can serve as valuable tools for testing relaxometry methods, it is important to emphasize that they do not replicate the complexity of biological tissue. For example, they do not accurately reproduce tissue properties such as relaxation anisotropy, which is observed in highly anisotropic tissues such as white matter. Previous studies have shown that T1 and T2 relaxation times in white matter are angle-dependent due to the orientation of axon fibers in the B_0 magnetic field [31–34]. This anisotropic nature of relaxation times cannot be mimicked by structurally homogenous phantoms.

Conclusion

This work shows that soy-lecithin-agar gels represents an alternative phantom material for the construction of relaxometry phantoms with tissue-like relaxation times, thus expanding the toolbox of qMRI-research. Soy-lecithin agar

gels are inexpensive, easy to prepare, and allow independent adjustment of T1 and T2 without marked susceptibility effects. With the presented manufacturing process, the relaxation times of almost all tissues can be mimicked, and without the use of toxic and/or paramagnetic substances.

Nevertheless, there are still open questions regarding the long-term stability and the temperature dependence of the phantoms which will be addressed in future studies.

Acknowledgements This work was supported and funded by the German Research Foundation (DFG) under grants SCHI 498/14-1, TH 1528/6-1 (package no. 997/1). It was furthermore supported in part by a grant (01GI0925) from the German Federal Ministry of Education and Research (BMBF) to the German Center for Diabetes Research (DZD e.V.)

Author contributions All authors contributed to the study conception and design. Study design and conception, material preparation, data collection and analysis were performed by [Fritz V]. [Eisele S] helped with the planning and production of the phantoms. [Martirosian P] and [Machann J] assisted with the MR measurements and analysis of data. [Schick F] conceived and supervised the project. The first draft of the manuscript was written by [Fritz V] in consultation with [Schick F]. All authors commented on previous versions of the manuscript and approved the final version for submission.

Funding Open Access funding enabled and organized by Projekt DEAL.

Declarations

Conflict of interest The authors declare that they have no conflict of interest.

Open Access This article is licensed under a Creative Commons Attribution 4.0 International License, which permits use, sharing, adaptation, distribution and reproduction in any medium or format, as long as you give appropriate credit to the original author(s) and the source, provide a link to the Creative Commons licence, and indicate if changes were made. The images or other third party material in this article are included in the article's Creative Commons licence, unless indicated otherwise in a credit line to the material. If material is not included in the article's Creative Commons licence and your intended use is not permitted by statutory regulation or exceeds the permitted use, you will need to obtain permission directly from the copyright holder. To view a copy of this licence, visit <http://creativecommons.org/licenses/by/4.0/>.

References

1. Keenan KE, Ainslie M, Barker AJ, Boss MA, Cecil KM, Charles C, Chenevert TL, Clarke L, Evelhoch JL, Finn P, Gembris D, Gunter JL, Hill DLG, Jack CR Jr, Jackson EF, Liu G, Russek SE, Sharma SD, Steckner M, Stupic KF, Trzasko JD, Yuan C, Zheng J (2018) Quantitative magnetic resonance imaging phantoms: A review and the need for a system phantom. *Magn Reson Med* 79(1):48–61
2. Stupic KF, Ainslie M, Boss MA, Charles C, Dienstfrey AM, Evelhoch JL, Finn P, Gimbutas Z, Gunter JL, Hill DLG, Jack CR, Jackson EF, Karaulanov T, Keenan KE, Liu G, Martin MN, Prasad PV, Rentz NS, Yuan C, Russek SE (2021) A standard

- system phantom for magnetic resonance imaging. *Magn Reson Med* 86(3):1194–1211
3. Stanisz GJ, Odobina EE, Pun J, Escaravage M, Graham SJ, Bronskill MJ, Henkelman RM (2005) T1, T2 relaxation and magnetization transfer in tissue at 3T. *Magn Reson Med* 54(3):507–512
 4. Cheng HL, Stikov N, Ghugre NR, Wright GA (2012) Practical medical applications of quantitative MR relaxometry. *J Magn Reson Imaging* 36(4):805–824
 5. Mitchell MD, Kundel HL, Axel L, Joseph PM (1986) Agarose as a tissue equivalent phantom material for NMR imaging. *Magn Reson Imaging* 4(3):263–266
 6. Kraft KA, Fatouros PP, Clarke GD, Kishore PR (1987) An MRI phantom material for quantitative relaxometry. *Magn Reson Med* 5(6):555–562
 7. Christofferson JO, Olsson LE, Sjöberg S (1991) Nickel-doped agarose gel phantoms in MR imaging. *Acta Radiol* 32(5):426–431
 8. Tofts PS, Shuter B, Pope JM (1993) Ni-DTPA doped agarose gel—a phantom material for Gd-DTPA enhancement measurements. *Magn Reson Imaging* 11(1):125–133
 9. Tofts PS (2003) QA: Quality Assurance, Accuracy, Precision and Phantoms. In: *Quantitative MRI of the Brain*. pp 55–81. <https://doi.org/10.1002/0470869526.ch3>
 10. Yoshimura K, Kato H, Kuroda M, Yoshida A, Hanamoto K, Tanaka A, Tsunoda M, Kanazawa S, Shibuya K, Kawasaki S, Hiraki Y (2003) Development of a tissue-equivalent MRI phantom using carrageenan gel. *Magn Reson Med* 50(5):1011–1017
 11. Kato H, Kuroda M, Yoshimura K, Yoshida A, Hanamoto K, Kawasaki S, Shibuya K, Kanazawa S (2005) Composition of MRI phantom equivalent to human tissues. *Med Phys* 32(10):3199–3208
 12. Hellerbach A, Schuster V, Jansen A, Sommer J (2013) MRI phantoms—are there alternatives to agar? *PLoS ONE* 8(8):e70343
 13. Vassiliou VS, Heng EL, Gatehouse PD, Donovan J, Raphael CE, Giri S, Babu-Narayan SV, Gatzoulis MA, Pennell DJ, Prasad SK, Firmin DN (2016) Magnetic resonance imaging phantoms for quality-control of myocardial T1 and ECV mapping: specific formulation, long-term stability and variation with heart rate and temperature. *J Cardiovasc Magn Reson* 18(1):62
 14. Altermatt A, Santini F, Deligianni X, Magon S, Sprenger T, Kappos L, Cattin P, Wuerfel J, Gaetano L (2019) Design and construction of an innovative brain phantom prototype for MRI. *Magn Reson Med* 81(2):1165–1171
 15. Gopalan K, Tamir JJ, Arias AC, Lustig M (2021) Quantitative anatomy mimicking slice phantoms. *Magn Reson Med* 86(2):1159–1166
 16. Woletz M, Roat S, Hummer A, Tik M, Windischberger C (2021) Technical Note: Human tissue-equivalent MRI phantom preparation for 3 and 7 Tesla. *Med Phys* 48(8):4387–4394
 17. Erdevig HE, Russek SE, Carnicka S, Stupic KF, Keenan KE (2017) Accuracy of magnetic resonance based susceptibility measurements. *AIP Adv* 7(5):1–6
 18. Panich AM (2022) Can detonation nanodiamonds serve as MRI phantoms? *MAGMA* 35(3):345–347
 19. Sekowska A, Majchrowicz D, Sabisz A, Ficek M, Bullo-Piontecka B, Kosowska M, Jing L, Bogdanowicz R, Szczerska M (2020) Nanodiamond phantoms mimicking human liver: perspective to calibration of T1 relaxation time in magnetic resonance imaging. *Sci Rep* 10(1):6446
 20. Fritz V, Martirosian P, Machann J, Daniels R, Schick F (2022) A comparison of emulsifiers for the formation of oil-in-water emulsions: stability of the emulsions within 9 h after production and MR signal properties. *MAGMA* 35(3):401–410
 21. Fritz V, Martirosian P, Machann J, Thorwarth D, Schick F (2023) Soy lecithin: A beneficial substance for adjusting the ADC in aqueous solutions to the values of biological tissues. *Magn Reson Med* 89(4):1674–1683
 22. Bojorquez JZ, Bricq S, Acquitter C, Brunotte F, Walker PM, Lalande A (2017) What are normal relaxation times of tissues at 3 T? *Magn Reson Imaging* 35:69–80
 23. Stikov N, Boudreau M, Levesque IR, Tardif CL, Barral JK, Pike GB (2015) On the accuracy of T1 mapping: searching for common ground. *Magn Reson Med* 73(2):514–522
 24. Sandle T (2019) Chapter 7—Selection and Application of Culture Media. In: Sandle T (ed) *Biocontamination control for pharmaceuticals and healthcare*. Academic Press, pp 103–123. <https://doi.org/10.1016/B978-0-12-814911-9.00007-9>
 25. Souza RM, Santos TQ, Oliveira DP, Souza RM, Alvarenga AV, Costa-Felix RPB (2016) Standard operating procedure to prepare agar phantoms. *J Phys: Conf Ser* 733(1):012044
 26. García-García R, Searle SS (2016) Preservatives: Food Use. In: Caballero B, Finglas PM, Toldrá F (eds) *Encyclopedia of Food and Health*. Academic Press, Oxford, pp 505–509. <https://doi.org/10.1016/B978-0-12-384947-2.00568-7>
 27. Israelachvili JN (2011) 2—Thermodynamic and Statistical Aspects of Intermolecular Forces. In: Israelachvili JN (ed) *Intermolecular and Surface Forces*, 3rd edn. Academic Press, San Diego, pp 23–51. <https://doi.org/10.1016/B978-0-12-375182-9.10002-8>
 28. Tadros TF (2013) Emulsion Formation, Stability, and Rheology. In: *Emulsion Formation and Stability*, pp 1–75. <https://doi.org/10.1002/9783527647941.ch1>
 29. Yu Z, Zhan J, Wang H, Zheng H, Xie J, Wang X (2020) Analysis of Influencing Factors on Viscosity of Agar Solution for Capsules. *J Phys: Conf Ser* 1653(1):012059
 30. Matzat SJ, McWalter EJ, Kogan F, Chen W, Gold GE (2015) T2 Relaxation time quantitation differs between pulse sequences in articular cartilage. *J Magn Reson Imaging* 42(1):105–113
 31. Schyboff F, Jaekel U, Petruccione F, Neeb H (2020) Origin of orientation-dependent R(1) (=1/T(1)) relaxation in white matter. *Magn Reson Med* 84(5):2713–2723
 32. Kauppinen RA, Thothard J, Leskinen HPP, Pisharady PK, Manninen E, Kettunen M, Lenglet C, Gröhn OHJ, Garwood M, Nissi MJ (2023) Axon fiber orientation as the source of T(1) relaxation anisotropy in white matter: a study on corpus callosum in vivo and ex vivo. *Magn Reson Med* 90(2):708–721
 33. Kauppinen RA, Thotland J, Pisharady PK, Lenglet C, Garwood M (2023) White matter microstructure and longitudinal relaxation time anisotropy in human brain at 3 and 7 T. *NMR Biomed* 36(1):e4815
 34. Knight MJ, Dillon S, Jarutyte L, Kauppinen RA (2017) Magnetic resonance relaxation anisotropy: physical principles and uses in microstructure imaging. *Biophys J* 112(7):1517–1528